Bull. Mater. Sci., Vol. 8, No. 2, May 1986, pp. 107–121. © Printed in India.

Computer calculations of phase diagrams

A K MALLIK
Indian Institute of Technology, Bombay 400076, India

Abstract. The thermodynamic route of establishing phase diagrams is a relatively recent activity, considering that till about the fifties most phase diagrams were determined by the measurement of certain physical property or quantitative microscopy using light optics or x-ray diffraction. The thermodynamic formalism used by Kaufman and Bernstein is explained and illustrated with examples of the development of hypothetical binary phase diagrams. The calculation of ternary phase diagrams can begin with the binary phase diagram data as a first approximation. However, to calculate a reasonably accurate ternary phase diagram a certain amount of ternary solution data is necessary. Various empirical equations have been proposed in the literature to express ternary thermodynamic data.

Calculation of simple ternary isothermal sections is illustrated with the examples of Mo-V-W and Cd-Sn-Pb systems. The numerical techniques which involve the differentiation of thermodynamic parameters with respect to composition get more involved with the number of components becoming 3 or more. A simpler approach has been applied recently to find the minimum position on the Gibbs free energy surface.

Keywords. Phase diagrams; solution models; binary diagrams; lattice stability; ternary diagrams; miscibility gap; hill climbing technique.

1. Introduction

A phase diagram represents the domains of stable phases under a given condition of composition and pressure. Till the fifties, phase diagrams were approached mainly through experimental measurements which did not involve thermodynamics, using either direct phase estimation methods or indirect methods. The indirect methods involve measurement of a physical property or rather a change thereof like dilation, resistivity etc or thermal analysis. The thermodynamics of phase equilibria represented, till about the fifties, a parallel activity with few bridges or connections with the former approach. As the stable state of a phase is associated with the minimum of free energy, it should be possible to link up thermodynamics with phase diagram, provided of course that an adequate representation of thermodynamic data is available. The reason why this link-up got going only after the fifties is perhaps due to the lack of communication between the physical chemists and physical metallurgists.

The relatively slow progress of the thermodynamic route to phase diagram has also been caused by the lack of data even for binary systems, not to speak of ternary systems. On the contrary, by the use of a physical property, phase diagrams can be determined directly. A natural consequence has been that "the number of systems for which phase diagrams have been determined is much greater than that for which the thermodynamic properties of solution phases are known" (Ansara 1979).

The situation has changed considerably during the last twenty five years and more and more phase diagrams are being generated from thermodynamic data. Not only does it provide considerable saving of labour but the exercise gives a deeper insight to the systematics of phase diagrams. The calculations have become feasible with the

availability of computers and appropriate numerical methods. Further, with the availability of sophisticated instruments, it has become possible to generate more precise and reliable thermodynamic data. Some of the early usage of thermodynamic data for the calculation of phase diagrams were by Wagner (1954), White *et al* (1977) and Hardy (1953). Extensive contributions have been made subsequently by Kubaschewski and Barin (1974), Kaufman and Bernstein (1970), Hillert (1970), Gaye and Lupis (1975), Chart *et al* (1975) and Pelton and Thompson (1975) on the calculation of phase diagrams. To conserve space, the mathematical formalism used in the present paper will be that of Kaufman and Bernstein, except where mentioned otherwise.

2. Phase equilibrium

At a given temperature and pressure, the maximum number of coexisting phases in a system formed by m components is equal to $(m+1)$ phases according to the phase rule. If there are j phases in the system, the partial free energy of a given component is the same for each phase under equilibrium conditions (figure 1). The condition can be expressed by a set of nonlinear equations such as

$$\bar{G}_i^{(1)} = \bar{G}_i^{(2)} = \bar{G}_i^{(j)}, \tag{1}$$

for $i = 1$ to mth element and 1 to jth phase. The equilibrium for a system is represented by the condition that the molar free energy is minimum.

3. Solution models

For an alloy system A–B, in which X represents the atom fraction of B and which exhibits two competing phases α and β, the free energies of each phase may be represented by the following equations

$$G^{\alpha} = (1-X)G_A^{\alpha} + XG_B^{\alpha} + \mathrm{RT}[X \ln X + (1-X)\ln(1-X)] + {}^{E}G^{\alpha}, \tag{2}$$

$$G^{\beta} = (1-X)G_A^{\beta} + XG_B^{\beta} + \mathrm{RT}[X \ln X + (1-X)\ln(1-X)] + {}^{E}G^{\beta}. \tag{3}$$

In (2) and (3) G_A^{α} and G_A^{β} are the free energies of the α and β modifications of the element A, while G_B^{α} and G_B^{β} are the free energies of the α and β modifications of the element B.

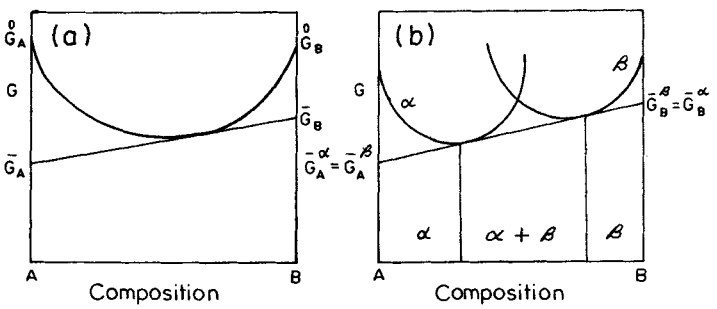

Figure 1. Common tangent construction to define equilibrium between two phases.

The excess free energies of mixing of the α and β phases are expressed as ${}^{E}G^{\alpha}$ and ${}^{E}G^{\beta}$ and X is the atom fraction of B.

The partial molar free energies of A and B in an alloy containing X atom fraction B are G_A and G_B respectively and are defined as

$$\bar{G}_A = G - X\frac{\partial G}{\partial X}, \tag{4}$$

$$\bar{G}_B = G + (1-X)\frac{\partial G}{\partial X}. \tag{5}$$

By differentiating G^{α} and G^{β} in (2) and (3) with respect to X, one can obtain the expressions for $\bar{G}_A^{\alpha}$, $\bar{G}_A^{\beta}$, $\bar{G}_B^{\alpha}$ and $\bar{G}_B^{\beta}$ i.e. the partial free energy terms. Further applying the concept of equality of chemical potentials as defined in (1), the following general equations can be obtained.

$$\Delta G_A^{\alpha\to\beta} + \mathrm{RT}\ln\left(\frac{1-X_\beta}{1-X_\alpha}\right) = \left({}^{E}G^{\alpha} - X\frac{\partial {}^{E}G^{\alpha}}{\partial X}\right) - \left({}^{E}G^{\beta} - X\frac{\partial {}^{E}G^{\beta}}{\partial X}\right), \tag{6}$$

$$\Delta G_B^{\alpha\to\beta} + \mathrm{RT}\ln\frac{X_\beta}{X_\alpha} = \left({}^{E}G^{\alpha} + (1-X)\frac{\partial {}^{E}G^{\alpha}}{\partial X}\right) - \left({}^{E}G^{\beta} + (1-X)\frac{\partial {}^{E}G^{\beta}}{\partial X}\right). \tag{7}$$

When ${}^{E}G = 0$, the solution is said to be ideal and the above equations can be considered simplified. Unfortunately, the ideal solution model is too simplistic and few solutions whether liquid or solid conform to it. A wide range of solution models have been suggested in the literature. However, in the present paper only the regular solution model will be used, which postulates that the ${}^{E}G$ term is equal to the enthalpy of mixing ΔH_m. For the regular solution model

$${}^{E}G^{\alpha} = E_\alpha X(1-X), \tag{8}$$

$${}^{E}G^{\beta} = E_\beta X(1-X), \tag{9}$$

where E_α and E_β are the interaction parameters for the α and β phases respectively. Equations (6) and (7) can now be simplified as

$$\Delta G_A^{\alpha\to\beta} + \mathrm{RT}\ln\left(\frac{1-X_\beta}{1-X_\alpha}\right) = E_\alpha X_\alpha^2 - E_\beta X_\beta^2, \tag{10}$$

$$\Delta G_B^{\alpha\to\beta} + \mathrm{RT}\ln\frac{X_\beta}{X_\alpha} = E_\alpha(1-X_\alpha)^2 - E_\beta(1-X_\beta)^2. \tag{11}$$

4. Numerical methods

Once the phase stability parameters $\Delta G_A^{\alpha\to\beta}$, $\Delta G_B^{\alpha\to\beta}$ and the interaction parameters E_α and E_β are estimated with some confidence, (10) and (11) can be solved by appropriate iterative procedures to obtain values for X_α and X_β, which make it possible to locate $\alpha|\alpha+\beta|\beta$ phase boundaries. Rudman (1969) used a trial and error method by assigning arbitrary values to the unknown X_α and X_β, so that the whole range of composition is covered. The values are then selected which best fit the equations. Kaufman and Bernstein (1970) used a method based on the Newton-Raphson iteration technique,

which will be briefly described here. This method involves selecting a couple of approximate equilibrium values for X_α and X_β as a starting point, from which more precise solutions are obtained using approximation computed as under

$$X_{\beta(n+1)} = X_{\beta(n)} - \frac{1}{(X_{\beta n}, X_{\alpha n})} \begin{vmatrix} F(X_{\beta n}, X_{\alpha n}) & F_{X\alpha}(X_{\beta n}, X_{\alpha n}) \\ G(X_{\beta n}, X_{\alpha n}) & G_{X\alpha}(X_{\beta n}, X_{\alpha n}) \end{vmatrix} \tag{12}$$

$$= X_{\beta(n)} - \frac{\Delta X_{\beta(n)}}{J(X_{\beta n}, X_{\alpha n})}$$

$$X_{\alpha(n+1)} = X_{\alpha(n)} - \frac{1}{J(X_{\beta n}, X_{\alpha n})} \begin{vmatrix} F_{X\beta}(X_{\beta n}, X_{\alpha n}) & F(X_{\beta n}, X_{\alpha n}) \\ G_{X\beta}(X_{\beta n}, X_{\alpha n}) & G(X_{\beta n}, X_{\alpha n}) \end{vmatrix}$$

$$= X_{\alpha(n)} - \frac{\Delta X_\alpha(n)}{J(X_{\beta n}, X_{\alpha n})}, \tag{13}$$

where $$F(X_\beta, X_\alpha) = 0,\ G(X_\beta, X_\alpha) = 0, \tag{14}$$

and the Jacobian

$$J(X_\beta, X_\alpha) = \begin{vmatrix} F'_{X\beta}(X_\beta, X_\alpha) & F'_{X\alpha}(X_\beta, X_\alpha) \\ G'_{X\beta}(X_\beta, X_\alpha) & G'_{X\alpha}(X_\beta, X_\alpha) \end{vmatrix}. \tag{15}$$

It can be seen that differentiation of thermodynamic properties with respect to the atomic fraction is involved and this becomes more difficult and involved as the number of components increases. They also have to be repeated for all expressions relating the free energy and atom fraction.

5. Binary diagrams

The utility of the Newton-Raphson iterative technique can be illustrated with the development of hypothetical binary phase diagrams reported by Balakrishna and Mallik (1979, 1980) and which are shown in figure 2. To begin with, simple isomorphous phase diagram is calculated when the solution is considered ideal. As the interaction parameters E_L and E_α are increased for the purpose of computation, the solidification range is enlarged and a solid state miscibility gap appears. Between the values of 4250 and 4500 cal/mol for the interaction parameters, an invariant peritectic reaction appears. By further raising the interaction parameter magnitude, a monotectic type reaction can be brought out.

The scope of the calculation can be illustrated further to deal with components exhibiting allotropy. Figure 3 shows the development of phase diagrams involving three phases, liquid (L) and solid phases (α) and (β), with varying combinations of the interaction parameters E_L, E_α and E_β. With small positive values of the interaction parameters, the equilibrium between L/β and β/α phases correspond to azeotropic minima. Increase of the value for E_α leads to the development of a miscibility gap in the α region. A further increase of E_α leads to the formation of an eutectoid reaction.

By suitably varying the relative magnitudes of the interaction parameters a wide range of phase diagrams can be generated. In real systems, however, the solid state interaction parameter will be greater than that of the liquid state. Further, by the very

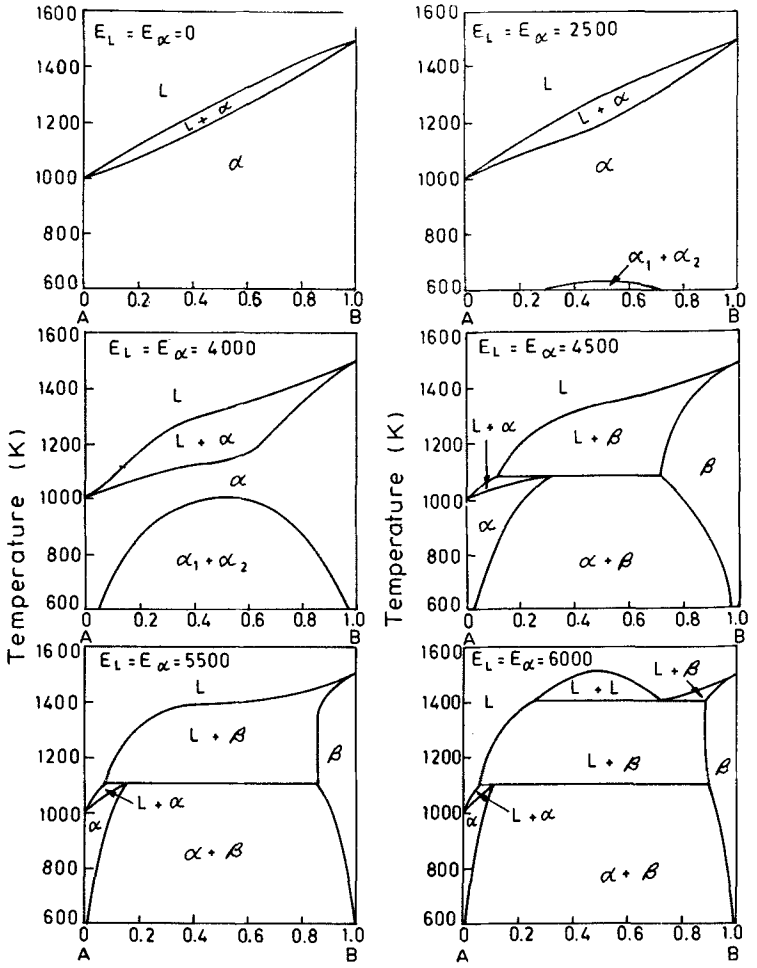

Figure 2. Development of peritectic and monotectic reactions with use of highly positive interaction parameters (cal/mol) (Balakrishna and Mallik 1979).

nature of formalism, the miscibility gaps so obtained are symmetrical. To deal with intermediate phases, in addition to the terminal phases, additional data are needed. Since there are many phase diagrams for which limited or very little thermodynamic data are available, it is quite possible to apply (10) and (11) in reverse, wherein the interaction parameters can be calculated using known values of X_α, X_β at the phase boundaries. The computed interaction parameters can be compared and averaged with available thermodynamic data to replot the phase diagram with more reliability (Appendix 1).

6. Lattice stability

To be able to determine the form of the free energy-composition curves, two important data are needed, which are the lattice stability and the free energy of mixing. While the

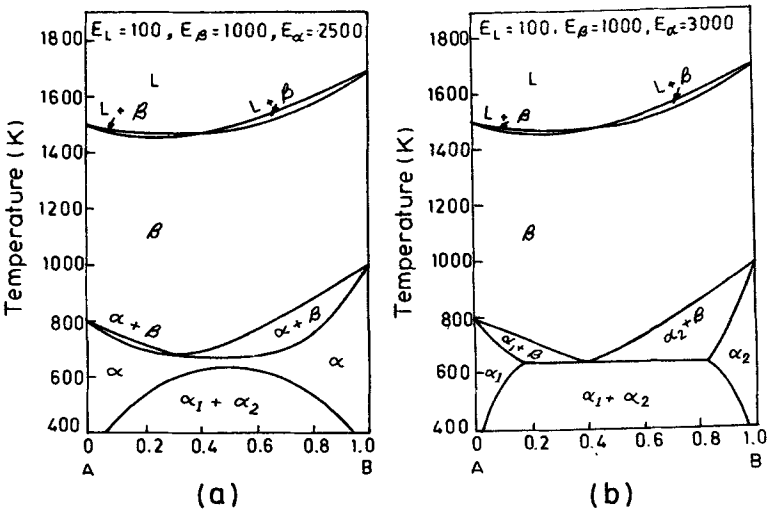

Figure 3. Development of phase diagrams with allotropy of both the components (interaction parameters in cal/mol) (Balakrishna and Mallik 1980).

relative shape of the curves is controlled by the latter, the former i.e. the lattice stability value controls the relative position of the free energy curves. Kaufman and Bernstein (1970) estimated the phase stability values for a number of elements, mainly transition metals, for different structural forms which are liquid, fcc, bcc and cph structures. The regular solution phase diagrams of 72 binary refractory metal systems were computed using the lattice stability values and computed interaction parameters.

While it would be ideal to obtain quantitative information on the lattice stability values from first principle formalism, such calculations are extremely difficult. If a metal exhibits polymorphism at atmospheric pressure, the free energy difference can be estimated from the measurements of the latent heat of transformation, heat of fusion and the volume changes attending the transformations. In cases where no polymorphism is displayed at one atmosphere, phase transformations at high pressures can be studied. The T-P diagram can be used with thermodynamic and volumetric data pertaining to one atmosphere to obtain the lattice stability expressions for various polymorphs. The analysis of phase diagram can enable the estimation of phase stability. For example, the lattice stability of hcp, fcc and bcc forms of Zn has been estimated through individual analysis of Al-Zn, Cu-Zn and Ag-Zn phase diagrams. Kaufman and Nesor (1978) and Kaufman (1978) published an extensive range of lattice stability values for a wide range of elements on coupled phase diagrams and thermochemical data.

7. Empirical equations for solutions

For the calculation of phase diagrams it is necessary to express the thermodynamic properties of multicomponent phases as analytical functions of composition. If no ternary data are available, the following representation for the excess integral free

energy may be used (Kohler 1960)

$$^{E}G = (1-X_A)^2\,{}^{E}G(BC) + (1-X_B)^2\,{}^{E}G(CA) + (1-X_C)^2\,{}^{E}G(AB) + \sum_{\substack{n\geq 1\\ m\geq 1\\ k\geq 1}} \phi_{nmk} X_A^n X_B^m X_C^k. \tag{16}$$

The three binary terms in (16) gives an exact representation of ^{E}G in the ternary system, if the ternary solution as well as all three binary solutions are regular and the ternary terms can be set to zero. An expression for the partial property $^{E}G_A$ corresponding to (16) may be derived by differentiation. Several other empirical equations have been proposed for expressing the thermodynamic properties of ternary systems which are shown in figure 4. Toop (1965) expressed the excess free energy of mixing for a ternary system by the following equation

$$^{E}G = \left[\frac{X_B}{1-X_A}\,{}^{E}G_{(AB)} + \frac{X_C}{1-X_A}\,{}^{E}G_{(AC)}\right] X_A + [(1-X_A)^2\,{}^{E}G_{(BC)}]X_B/X_C \tag{17}$$

The equations given by Toop (1965) and Kohler (1960) have also been used with an additional term of the form $X_A X_B X_C\,(AX_A + BX_B + CX_C + D)$ to represent experimental data, the coefficients A, B, C and D being calculated from a least square analysis. Pelton and Bale (1977) represented the integral molar excess free energy E at any constant temperature for the ternary system (Bi-Cd-Zn) by a general polynomial expansion as given below

$$^{E}G = \Sigma\, \phi_{nmk} X_{\mathrm{Zn}}^n X_{\mathrm{Cd}}^m X_{\mathrm{Bi}}^k, \tag{18}$$

where the ϕ_{nmk} are constant coefficients. Any number of terms necessary to adequately represent the system may be included. Expressions for the partial molar excess free

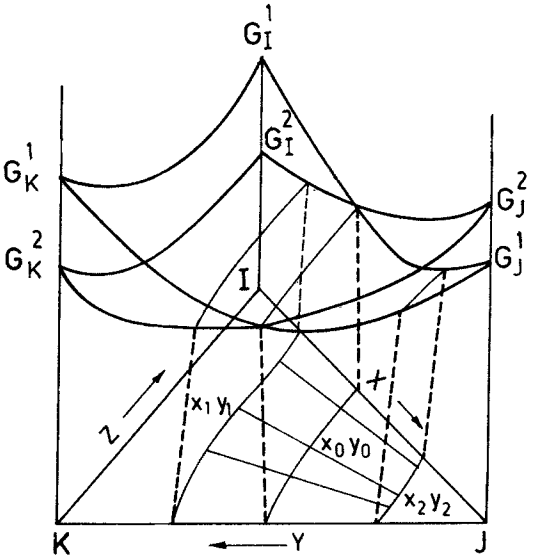

Figure 4. Free energy surfaces of competing phases in ternary system and application of the common tangent principle.

energy may be obtained by differentiation of (18). Using the above formalism Pelton and Bale (1977) calculated the phase diagrams for the Bi-Cd-Zn, Bi-Cd-Sn and Fe-Cr-Ni-O systems.

8. Ternary diagrams

The formalism reported for the binary system can be extended to the ternary system. The integral free energy of a single phase solution with 3 components can be expressed as (Kaufman and Bernstein 1970)

$$G[X,Y,T] = ZG_i + XG_j + YG_k + \mathrm{RT}(Z\ln Z + X\ln X + Y\ln Y) + XZE_{ij} + YZE_{ik} + XYE_{jk}, \tag{19}$$

where X, Y, Z are atomic fraction of elements J, K and I respectively, G_i, G_j, G_k the free energies of the pure element I, J, K and E_{ij}, E_{ik} and E_{jk} are the binary interaction parameters.

The partial free energies of I, J, K in a given phase are

$$\bar{G}_i = G - X\frac{\partial G}{\partial X} - Y\frac{\partial G}{\partial Y},$$

$$\bar{G}_j = G + (1-X)\frac{\partial G}{\partial X} - Y\frac{\partial G}{\partial Y},$$

$$\bar{G}_k = G - X\frac{\partial G}{\partial X} + (1-Y)\frac{\partial G}{\partial Y}. \tag{20}$$

The equilibria between two phases, liquid (L) and solid (S) can be shown schematically by the common tangent plane in figure 4, which shows the locus of points (X_1, Y_1) and (X_2, Y_2) corresponding to possible tangent points of a plane tangent to the two free energy surfaces $G^1[X,Y,T]$ and $G^2[X,Y,T]$. As with the binary diagrams and equations (10) and (11), similar equations can be written for the ternary case as

$$\begin{aligned}
A_i &= \Delta G_i^{1\to 2} + \mathrm{RT}\ln(Z_2/Z_1) + (E_{ij}^2 X_2^2 - E_{ij}^1 X_1^2) + (E_{ik}^2 Y_2^2 - E_{ik}^1 Y_1^2) \\
&\quad + (\Delta E^2 X_2 Y_2 - \Delta E^1 X_1 Y_1) = 0, \\
A_j &= \Delta G_j^{1\to 2} + \mathrm{RT}\ln(X_2/X_1) + [E_{ij}^2(1-X_2)^2 - E_{ij}^1(1-X_1)^2] \\
&\quad + (E_{ik}^2 Y_2^2 - E_{ik}^1 Y_1^2) - [\Delta E^2 Y_2(1-X_2) - \Delta E^1 Y_1(1-X_1)] = 0, \\
A_k &= \Delta G_k^{1\to 2} + \mathrm{RT}\ln(Y_2/Y_1) + (E_{ij}^2 X_2^2 - E_{ij}^1 X_1^2) + [E_{ik}^2(1-Y_2)^2 \\
&\quad - E_{ik}^1(1-Y_1)^2] - [\Delta E^2 X_2(1-Y_2) - \Delta E^1 X_1(1-Y_1)] = 0,
\end{aligned} \tag{21}$$

where $$\Delta E = E_{ij} + E_{ik} - E_{jk}. \tag{22}$$

Equation (21) is solved numerically by the Newton-Raphson iteration technique (Appendix 2).

For starting the iteration one has to choose the initial value of X_1 for the independent variable and then choose the starting values of X_2^0, Y_1^0, Y_2^0. As shown in figure 5 the two binary edges IJ and JK define limits of $X_1 Y_1$ and $X_2 Y_2$. The iteration is continued until it converges on a solution of X_2, Y_1, Y_2. The value of X_1 is then changed slightly and the procedure is repeated using previous solutions found for X_1. The correctors

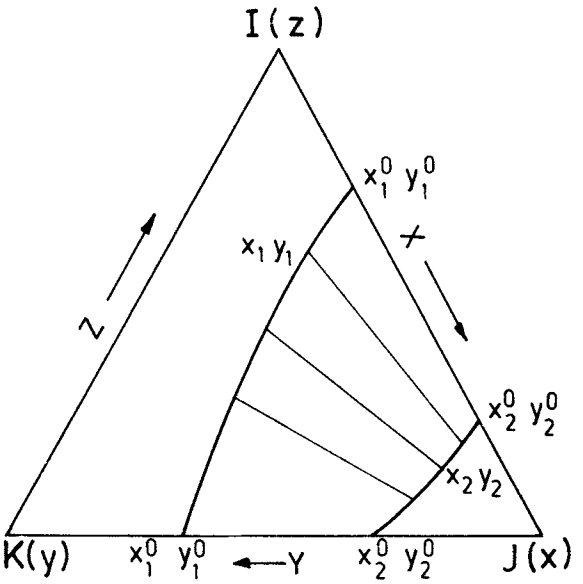

Figure 5. Computation of phase boundaries and tie lines with isothermal ternary sections from *IJ* edge to the *JK* edge.

ΔX_2, ΔY_1, ΔY_2 in the determinant form are

$$J\Delta X_2 = \begin{vmatrix} -A_i\dfrac{\partial A_i}{\partial Y_1} & \dfrac{\partial A_i}{\partial Y_2} \\ -A_j\dfrac{\partial A_j}{\partial Y_1} & \dfrac{\partial A_j}{\partial Y_2} \\ -A_k\dfrac{\partial A_k}{\partial Y_1} & \dfrac{\partial A_k}{\partial Y_2} \end{vmatrix},$$

$$J\Delta Y_1 = \begin{vmatrix} \dfrac{\partial A_i}{\partial X_2} - A_i\dfrac{\partial A_i}{\partial Y_2} \\ \dfrac{\partial A_j}{\partial X_2} - A_j\dfrac{\partial A_j}{\partial Y_2} \\ \dfrac{\partial A_k}{\partial X_2} - A_k\dfrac{\partial A_k}{\partial Y_2} \end{vmatrix},$$

$$J\Delta Y_2 = \begin{vmatrix} \dfrac{\partial A_i}{\partial X_2}\dfrac{\partial A_i}{\partial Y_1} - A_i \\ \dfrac{\partial A_j}{\partial X_2}\dfrac{\partial A_j}{\partial Y_1} - A_j \\ \dfrac{\partial A_j}{\partial X_2}\dfrac{\partial A_k}{\partial Y_1} - A_k \end{vmatrix}, \tag{23}$$

where J, the Jacobian determinant is

$$J = \begin{vmatrix} \frac{\partial A_i}{\partial X_2} & \frac{\partial A_i}{\partial Y_1} & \frac{\partial A_i}{\partial Y_2} \\ \frac{\partial A_j}{\partial X_2} & \frac{\partial A_j}{\partial Y_1} & \frac{\partial A_j}{\partial Y_2} \\ \frac{\partial A_k}{\partial X_2} & \frac{\partial A_k}{\partial Y_1} & \frac{\partial A_k}{\partial Y_2} \end{vmatrix}. \tag{24}$$

8.1 *Calculated phase diagrams*

Figure 6 shows the calculated isothermal section for the Mo-V-W system by Bhansali and Mallik (1984) using the above approach, for which experimental diagram is not available. All the binaries are of the isomorphous type with complete solid solubility. Both ideal and regular solution models have been used. It may be noted that while the

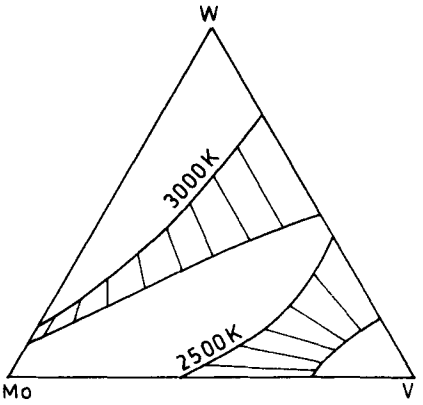

Figure 6. Calculated isothermal sections for the Mo-V-W ternary phase diagram (Bhansali and Mallik 1984).

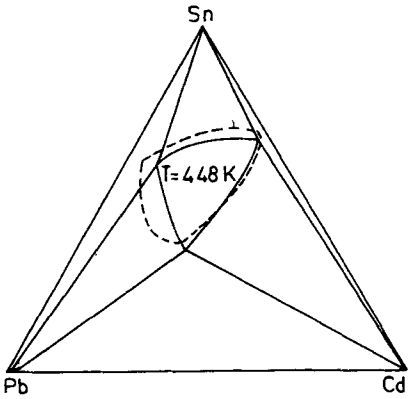

Figure 7. Calculated isothermal sections for the Cd-Pb-Sn ternary phase diagram (Bhansali and Mallik 1984) - - - experimental.

ideal solution model produces almost straight liquidus and solidus lines, the regular solution model produces more realistic contours which are naturally curved.

Figure 7 shows the calculated liquidus projections for the ternary system Cd-Pb-Sn, (Bhansali and Mallik 1984) which shows one eutectic reaction at each of the binary edges. The figure also shows experimental lines obtained by thermal analysis and the match between experimental and computed lines is rather satisfactory. This is so considering that only binary phase diagram data have been used in the calculation of this diagram. Two alternatives are available. The first is to use calculated binary interaction parameters. The second is to use interaction parameters which are manipulated to produce the best fit with the binary diagram. In the above ternary phase diagrams the second alternative has been used. It is further possible to introduce ternary interaction parameters. This is where some measurements of thermodynamic data in the ternary region can be extremely useful.

8.2 *Ternary miscibility gap*

The magnitudes of the interaction parameters indicate the extent of solubility or immiscibility. Positive interaction parameter represents repulsive interaction between the two atomic species in solution. If the binary interaction parameter exceeds 2RT a miscibility gap is expected, which may or may not extend to the other binary edge depending on the magnitude of the other binary interaction parameter. The problem of defining the phase boundaries is similar to the two solution phase situation. The schematic free energy surface is shown in figure 8, which shows the occurrence of miscibility gaps on IJ and IK binary edges. Equation (21) can be used with the modification that $\Delta G_i^{1\to 2} = 0$, $E_{ij}^1 = E_{ij}^2 = E_{ij}$. In case only one binary shows the miscibility gap the upward convexity of the free energy surface will gradually disappear as one moves from one binary edge to the other.

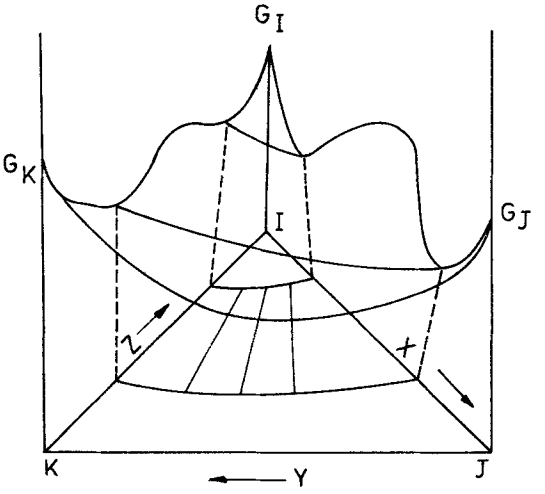

Figure 8. Schematic representation of the free energy surface for miscibility gaps at two binary edges.

9. Hill climbing technique

It has been pointed out that the differentiation of thermodynamic properties with respect to atomic fraction becomes more difficult and cumbersome as the number of components increases beyond three. The problem becomes even more difficult if there are small erroneous inflexions in the free energy curve determined from experimental observations. Nelder and Mead (1965) suggested a simplex approach which finds the minimum positions on the Gibbs free energy surface by hill climbing computational technique. In this method, the free energy of a multicomponent system is calculated at a certain number of coordinates, usually 10. The point which has the highest value of free energy is replaced by another one. The procedure is iterated until a minimum value is obtained. This technique has been used by Counsell *et al* (1971) to calculate the miscibility gap in the liquid Cd-Pb-Zn and Cd-Pb-Sn-Zn systems. The method can also be used when tables of discrete values of thermodynamic data are used in place of analytical expressions. The minimization of free energy has been tested for two-phase separation in binary, ternary and quaternary mixtures. The procedure can be used to minimize a function of m variables by comparison of the values of this function at $m+1$ points, followed by replacement of the point corresponding to the highest value of the function by another point. The process is continued by reflection, contraction and expansion upto the point when a minimum value is obtained.

10. Higher order phase diagrams

A quarternary phase diagram is usually represented as a regular tetrahedron, where the four equilateral triangular surfaces represent the 4 ternary diagrams and the six edges represent 6 binary diagrams at a given temperature. The lattice simplex method has been used (Ansara 1979) to express mathematically liquidus or solidus volumes in higher order systems. In principle, the method (Scheffe 1958; Gorman and Hinman 1962) involves constructing mathematical models, commonly polynomials, which correlate the property and composition of test alloys. To calculate the coefficients of the equations, the properties are measured according to a definite distribution within a simple lattice. Relatively few quarternary systems have been investigated in detail.

11. Conclusions

The calculation of binary phase diagrams has been actively pursued in the last 25 years. While adequate description exists for the terminal phases (bcc, fcc and hcp forms), phase diagrams with several intermediate phases can only be attempted with some experimental data about their stability. The regular solution model, notwithstanding its limitations has been used quite extensively.

For the calculation of ternary phase diagrams the starting point can be the binary system data. Analytical series expansions have been developed for representing the thermodynamic data of ternary and higher order solutions as a function of composition. A major uncertainty relates to the extension of the binary intermediate phases into the ternary regions. Asymmetrical miscibility gaps also cannot be determined without some data.

Such computational techniques which use the differentiation of thermodynamic parameters with respect to composition become more difficult beyond ternary diagrams. Thus, use of other minimization techniques, which do not involve differentiation may be more attractive. As yet, the calculation of quarternary phase diagrams has been attempted on a limited scale only.

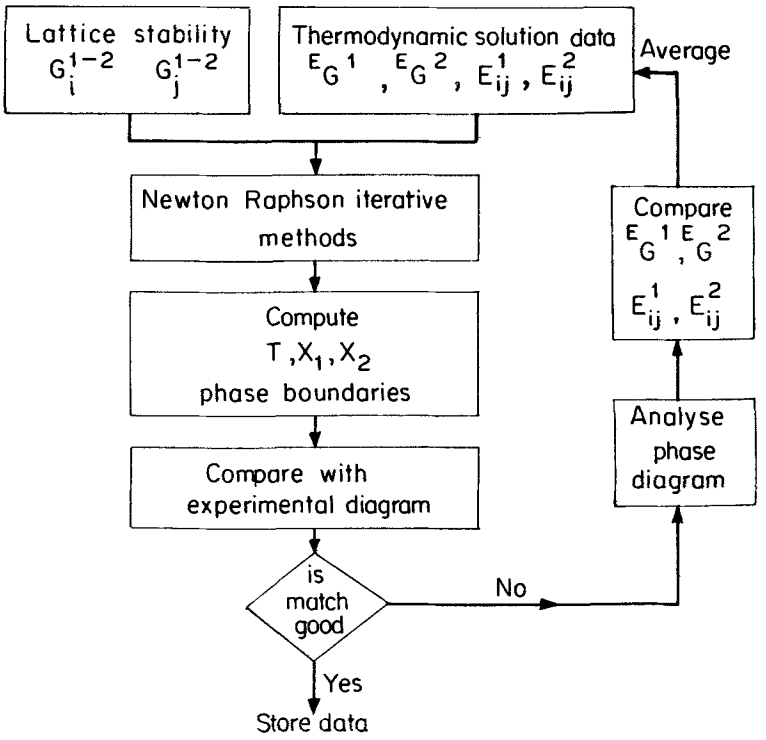

Appendix 1. Flow diagram for coupling of thermodynamic data with phase diagram data for the generation of averaged phase diagram.

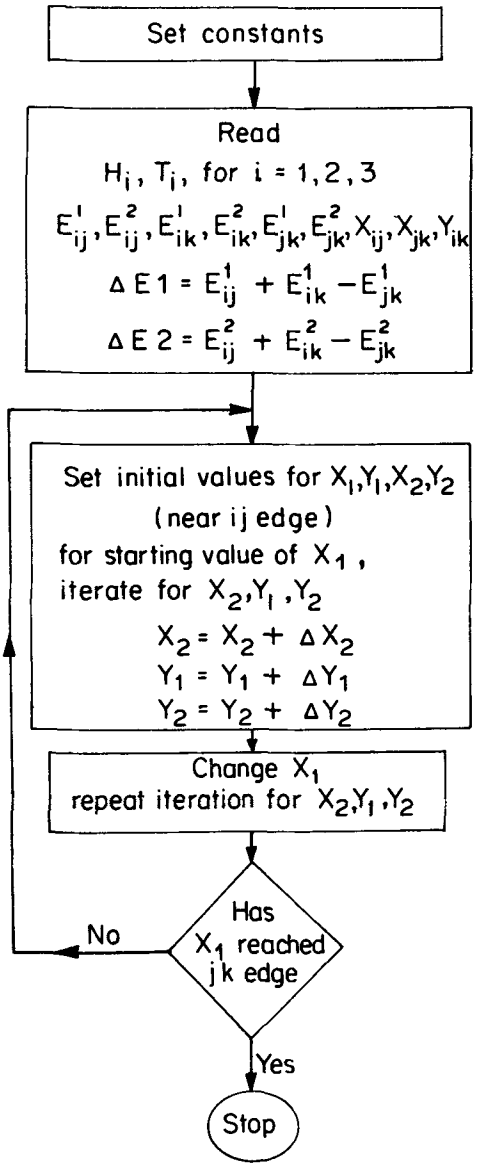

Appendix 2. Flow diagram for the iterative calculation of phase boundaries in ternary diagram isothermal sections.

References

Ansara I 1979 *Int. Metall. Rev.* **238** 20
Balakrishna S S and Mallik A K 1979 ICMS-77 Varanasi, Indian Inst. of Met, Varanasi p. 107
Balakrishna S S and Mallik A K 1980 *Trans. Indian Inst. Met.* **33** 155
Bhansali A and Mallik A K 1985 (Communicated)
Counsell J F, Lees E B and Spencer P J 1971 *Met. Sci. J.* **5** 210
Chart T G, Counsell J F, Jones G P, Slough W and Spencer J P 1975 *Int. Metall. Rev.* **20** 57

Gaye H and Lupis C H P 1975 *Metall. Trans.* **4** 685
Gorman L W and Hinman J E 1962 *Technometrics* **4** 463
Hardy H K 1953 *Acta Metall.* **1** 202
Hillert M 1970 *Phase transformations* (Ohio: Am. Soc. for Metals)
Kohler F 1960 *Monatsh. Chem.* **91** 738
Kaufman L and Bernstein H 1970 *Computer calculations of phase diagrams* (New York: Academic Press)
Kubaschewski O and Barin I 1974 *Pure Appl. Chem.* **38** 469
Kaufman L and Nesor H 1978 CALPHAD (*Computer coupling of phase diagrams and thermochemistry*) **2** 81
Kaufman L 1978 CALPHAD (*Computer coupling of phase diagrams and thermochemistry*) **2** 117
Nelder J A and Mead R 1965 *Comput. J.* **7** 308
Pelton A D and Bale C W 1977 CALPHAD (*Computer coupling of phase diagrams and thermochemistry*) **1** 253
Pelton A D and Thompson W T 1975 *Prog. Solid State Chem.* **10** 119
Rudman P S 1969 *Advances in materials research* (New York: Interscience) Vol. 4
Scheffe H 1958 *J. R. Stat. Soc.* **B20** 344
Toop G W 1965 *Trans. Metall. Soc.* AIME, **233** 850
Wagner C 1954 *Acta Metall.* **2** 242
White J L, Orr R L and Hultgren R 1977 *Acta Metall.* **5** 747